On the overlooked impact of river dams on beach erosion worldwide

Graffin M.[1,2], **Regard V.**[1], **Almar R.**[2], **Carretier S.**[1], **Maffre P.**[3]
Correponding author : Marcan Graffin (marcan.graffin@etu.toulouse-inp.fr)

The paper is a non-peer reviewed preprint draft submitted to EarthArXiv.
The manuscript is currently undergoing peer review for the journal **Nature Sustainability**.

Abstract

The current retreat of the world's coastline has a profound impact on human activities and ecosystems. The scientific community has primarily focused on the potential impact of sea level rise. At the global scale, the contribution of river sand loads to coastal erosion has been overlooked. Here we present the first global sand pathway model from land to sea. Our model reveals that sand tends to accumulate towards tropical regions. We show that the recent shoreline evolution is significantly controlled by the imbalance in the sand budget, challenging the idea that sea level rise due to climate change is currently the main driver of coastal erosion. Our model highlights that the significant reduction in sand supply due to tens of thousands of river dams and its consequences on coastal erosion could be avoided by an effective sustainable management policy.

Introduction

Coastal zones are dynamic areas at the interfaces between land and sea. These areas concentrate a large part of the world's population as well as rich and rare ecosystems. However, human activity severely affects the fragile equilibrium of these areas, notably by influencing the climate and ecological continuity, thereby weakening coastal ecosystems while increasing the exposure of populations to natural hazards [1].

Sandy beaches in low-lying coastal areas are currently undergoing particularly dramatic erosion that is destabilizing coastal socio-ecosystems [2]. In spite of the economic, cultural and environmental interest of coastal zones, the scientific literature makes little mention of the global drivers of coastline evolution. It is generally assumed *a priori* that global and regional oceanic factors such as sea level rise and changes in wave regimes are the primary drivers of beach evolution [3, 4, 5, 6, 7], predicting unprecedented future beach retreat and disappearance [8]. However, the magnitude of the retreat and the importance of other factors driving beach changes are currently being debated [9], in particular oceanographic and geologic processes over a wide range of spatial and temporal scales, all affected by climate and human factors in diverse ways. These processes include sea level changes, sediment transport by tides, currents and waves, sediment supply from rivers and land and offshore loss, and coastal uplift or subsidence, among many others [10]:

$$\text{Coastline Evolution} = function(\text{Nearshore Transport}, \text{Sources}, \text{Sinks}, \text{Relative Sea Level}) \quad (1)$$

There is a permanent flow of sediment from watersheds to the ocean, delivered by rivers. Sand grains are deposited at the coast by rivers, while the finer sediment particles are carried further out to sea. Thus, sand that has been temporarily deposited in the nearshore area around the river outlet is then resuspended by waves. The one-way longshore transport ends when the sand permanently deposits in the nearshore system or when it flows into a submarine canyon and permanently leaves the nearshore system. A nearshore hydrosedimentary cell is a distinct area of coastline where sand enters the ocean and flows along the coast in a single direction. At the convergence of two successive cells, sand can either accumulate or be removed from the system. The balance of sand available for beaches is the amount of sand entering the littoral cell minus the amount leaving. If this sand balance is altered, the beach morphology changes.

[1]GET (Université de Toulouse/CNRS/IRD/UPS), Toulouse, France
[2]LEGOS (Université de Toulouse/CNRS/IRD/UPS), Toulouse, France
[3]University of Berkeley, San Francisco, California, The U.S.A

Recently, Nienhuis et al. [11] highlighted the role of river sediment supply for 1000 deltas worldwide who have been subjected to land loss due to dam building. The proliferation of river and coastal infrastructures hinders sediment transit and contributes to depriving beaches located away from outlets of an essential supply of sand [12] while deltas[11],[13] and estuaries[14] are more likely to accrete. At the same time, the sea level rise will accelerate[15] at an unprecedented rate that will compound the current problems.

Coastal sand pathways at the global scale have not been addressed by the scientific community as of yet. There is a need for a comprehensive consideration of sand availability as a driver of global coastlines[16]. Given that satellite observations are now abundant[17, 18], such global studies can be performed. Luijendik et al.[2] analysed thousands of satellite-based shoreline data from 1984 to 2016; they found that 31% of the world's ice-free shoreline are sandy, among which 24% are eroding, 28% are accreting and 48% are stable. In order to predict sandy coast erosion and accretion [8], there is still a need to develop numerical models based on observations and physical processes[19]. This is the way forward to improve science-based coastal management strategies so as to effectively mitigate the effect of the inevitable sea level rise due to climate change as well as human interventions on the sediment pathway[20].

Here, we investigate how the combination of terrestrial sand supply and sand coastal redistribution drive the coastline evolution at the global scale. We introduce a new integrated sand pathway model, and we quantify the impact of dams on modern era coastal sand budgets and the observed coastline retreat.

Our global sand pathway model

A numerical 'along-coast' sand transport model has been developed and implemented on a global scale along the coastline which has been segmented into 50 km-long transects. The sand budget of each one of the 11,161 calculated transects is defined considering the sand mass conservation equation defined above(Figure 1) calculated nearshore from one end of the transect to the other and from the coast to the depth of closure. The source term corresponds to the solid discharge by rivers (referred to then as Q_{river})[21], and the sink term corresponds to the cross-shore sand transport towards the deep ocean[22, 23, 24]. Last, a transfer term corresponds to the wave-induced longshore sand transport (referred then as Q_{wave})[25]. It is the predominant factor in the transport of sand along open coasts exposed to waves, reaching its maximum in the surf zone which generally extends offshore for tens of metres to kilometres. Each of these sediment fluxes relies on different physical mechanisms and thus requires a large amount of data to be estimated. Q_{river} is calculated from a calibrated erosion law (BQART formula) depending on the catchment area, mean annual catchment discharge, average temperature and local slope[26, 27] (Methods). Q_{wave} is calculated from ocean data such as the wave period, wave orientation relative to the coast and the breaking wave height [25] (Methods). The cross-shore sand transport is estimated from the local depth of closure. The depth of closure is the maximum depth of significant seaward cross-shore sediment transport by the waves; it provides information on the fraction of sand flux leaving the coastal system toward the open ocean[23] (Figure 1).

This model predicts patterns in coastal sand accumulation and removal, i.e. accreted or eroded volumes. We do not predict sandy coast growth or retreat, strictly speaking, because in order to convert the calculated accumulation/removal volumes into morphological evolution this would require taking into account the relative sea level changes (e.g. sea level rise, subsidence) and morphodynamic considerations (e.g. beach profile evolution), which would then add unnecessary uncertainties for the specific question addressed in this contribution.

Tropical sandy beaches resulting from a global convergence of wave-driven sand transport?

The quantification of Q_{river} is well documented locally at the outlets of the world's major rivers[21]. It is then possible to integrate over large areas (e.g. continent) and on the global scale [21, 27]. Using the BQART formula at the global scale gives a total annual sediment flux of $\Sigma\ Q_{river} = 15.1\ Gt/yr$, within the range of current estimates[28, 29], corresponding to $5700 \times 10^6\ m^3/yr$ - considering $\rho_s = 2650\ kg/m^3$. Spread over all the coastal transects, this gives an average of 1,050,000 tons per year per transect, or 400,000 cubic metres per year per transect.

The time-averaged Q_{wave} obtained from oceanic conditions is an estimate of the potential (i.e. maximum) annual flux of sediment transport along the coast by waves. On a global scale, the longshore sediment transport is structured into coastal cells (e.g. mainland, islands) along which sediments flow in the same direction. Changes in sediment supply affect the entire cell. On average, the longshore sediment transport potential is approximately 155,000 cubic metres (410,000 tonnes) per year, which is the same order of magnitude as the average Q_{river}. This similarity means that the longshore transport capacity can globally convey the river input from their outlet all around the coastal cells, leading to sediment accumulation at the boundary between two adjacent cells, where longshore sediment transport converges. The global latitudinal means of Q_{wave} show the tendency of waves in the northern and southern hemispheres to transport sediment southward or northward, respectively. Around the equator, the reversal of the direction of the longshore sediment transport potential represents a global convergence zone of these transport potentials. On average, on a global scale, waves induce sediment transport from higher latitudes to the equatorial zone with notably high sediment deposition in tropical areas where the decrease in wave

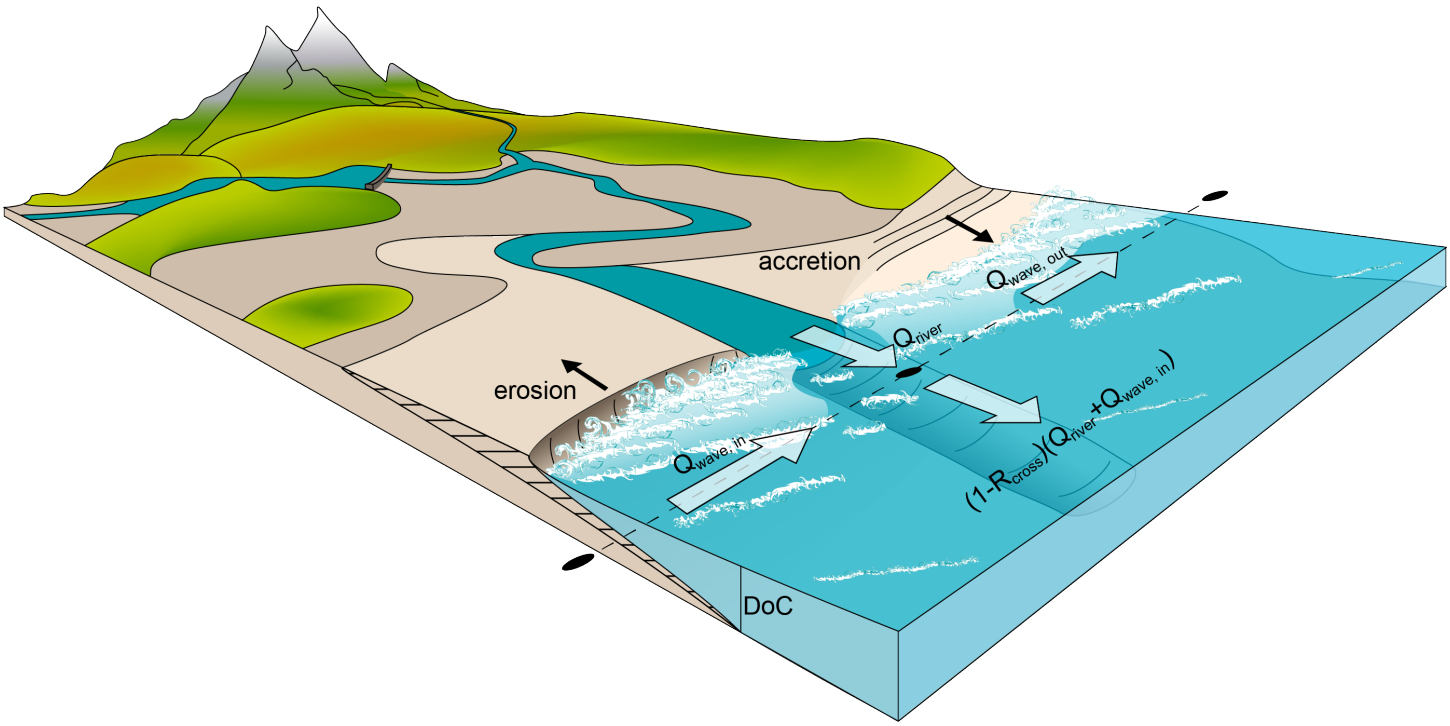

Figure 1: **Schematic representation of the model.** Schematic diagram of the sand budget at the coast for one transect (centred on one black ellipse). The influx of sand comes from the river (Q_{river}) as well as the wave-induced longshore drift ($Q_{wave,in}$). Conversely, sand is lost by the longshore drift ($Q_{wave,out}$), or the cross-shore sediment transport fraction (R_{cross}). A positive or negative budget is indicative of accretion or erosion at the coast, respectively.

activity is most pronounced. (Figure 2).

Figure 2c illustrates that the relative importance of $\mid Q_{wave} \mid$ and Q_{river} depends on the latitude. Between 15°N and 5°S, Q_{river} dominates over $\mid Q_{wave} \mid$ whereas $\mid Q_{wave} \mid$ dominates south of 10°S and north of 35°N.

When $Q_{river} <\mid Q_{wave} \mid$, the river sediment supply is easily transported away by Q_{wave}. Sediment deposition, e.g. beach construction, is expected where $\mid Q_{wave} \mid$ diminishes. On the contrary, areas where $Q_{river} >\mid Q_{wave} \mid$ may be dominated by large river sediment discharge, and locally outweighs Q_{wave}, which means that most of the sediment input is either deposited near the outfall or it drifts out to sea.

From 25°N to 0° (30°S to 0°), there is a consistent gradient in the mean southward (northward) coastal transport, which means that the southern (northern) component of coastal transport tends to decrease progressively from 25°N to 0° (30°S to 0°). This gradient of transport capacity leads to a progressive deposition of sediments, especially in tropical areas where this trend is the most pronounced.

At low latitudes (as well as in enclosed seas), the weak wave regime induces a shallow depth of closure[30], which greatly limits the size of the nearshore zone. Consequently, sediment is more likely to bypass or drift directly from river outlets into the open ocean[31]. In our model, this results in low values of R_{cross} at the equator, which lead to low sand budgets despite high riverine inputs.

These predictions of the distribution of sandy beaches are consistent with observations made from satellite observations by *Luijendijk et al.*[2], and thus provide a first explanation for the increased presence of beaches in tropical zones.

River sand supply as the overlooked driver of the modern era global beach evolution

Unlike relative sea level rise, sand supply is rarely mentioned as being potentially responsible for beach erosion dynamics on a global scale. However, it appears that many coastal sites in the world are subjected to erosion that extends well beyond the relative rise in sea level, such as the deltas of large rivers, which are deprived of a significant part of their sediment supply by dams and irrigation networks[11, 32, 33].

In order to quantify the influence of sand input on beach dynamics and to evaluate the sand distribution model, we compare our results with observed coastline evolution data. As no sand budget database exists on a global scale, we use the shoreline evolution data from *Luijendijk et al.*[2] as a proxy. After having automatically extracted the global spatial distribution of beaches, *Luijendijk et al.*[2] analysed the annual evolution trend of the coastline (v_{obs} in $m/year$) and the yearly variability of the observations around this trend (ϵ_{obs}). Note that from now on, our analysis is restricted to the beach

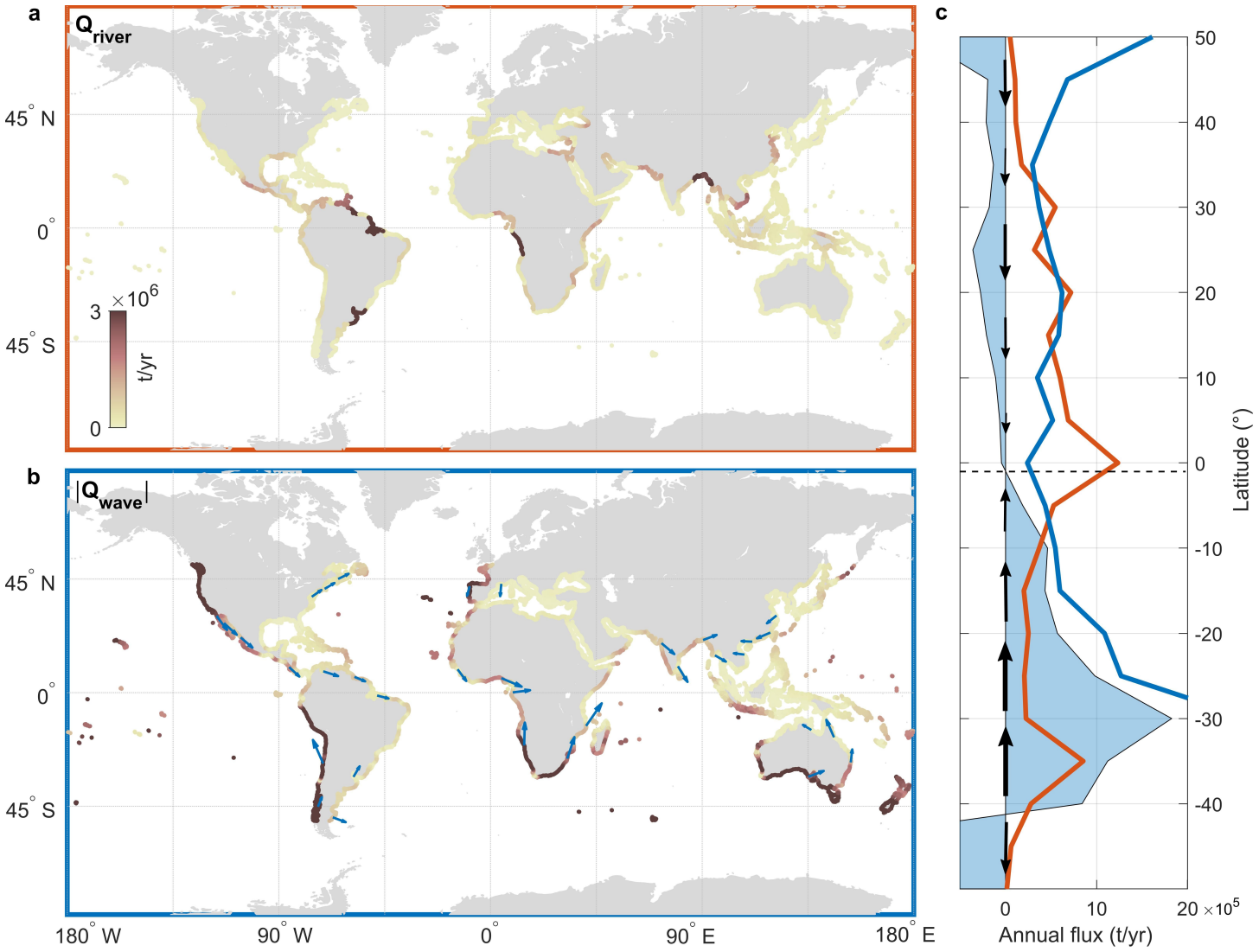

Figure 2: **A global view of fluvial sediment supply and longshore sediment transport.** (**a**) Global geographic distributions of the river sediment discharge (Q_{river}) and (**b**) absolute longshore sediment transport potential (| Q_{wave} |), with arrows indicating the direction of transport and circles showing the major convergence areas. (**c**) 5° resolution latitudinal averages of Q_{river} (red line), absolute Q_{wave} (blue line) and Q_{wave} (blue polygons - positive for northward oriented, negative for southward oriented). Black arrows show the direction and intensity of the long-shore sediment transport.

areas contoured by *Luijendijk et al.*[2], which represents roughly one third of the entire transect dataset.

In order to isolate the role of the imbalance in the sand budget from that of continuous mechanisms such as sea level rise or subsidence, we focus on ϵ_{obs}. This variability corresponds to high frequency events (intra to inter-annual), and therefore cannot be due to mechanisms acting on decadal time scales such as continuous sea level rise or land subsidence. We postulate that this variability instead reflects variations in the sediment imbalance at a local scale, due to a competition between Q_{river} and Q_{wave}.

For the subset of sandy transects where this assumption seems to be true (see Methods), which represents 64% of the sandy coastlines of the *Luijendijk et al.*[2] database, the correlation coefficient between v_{obs} and ΔQ is $R = 0.588$. The imbalance of the sand budget thus explains half of the variance of the coastal erosion trends for 64% of the transects provided by *Luijendijk et al.*[2]. We observed either no correlation or a weaker correlation when considering the entire dataset and when rocky and sandy coasts are not differentiated ($R = 0.381$, Table 1 in Methods).

The significant correlation $R = 0.588$ between ΔQ and v_{obs} for a large majority of global sandy beaches shows that our sand budget model captures a first order contribution to the current sandy coastline evolution. This contribution is the local imbalance of coastal sediment flux. Thus, the river sediment supply cannot be neglected when considering the evolution of beaches at a global scale.

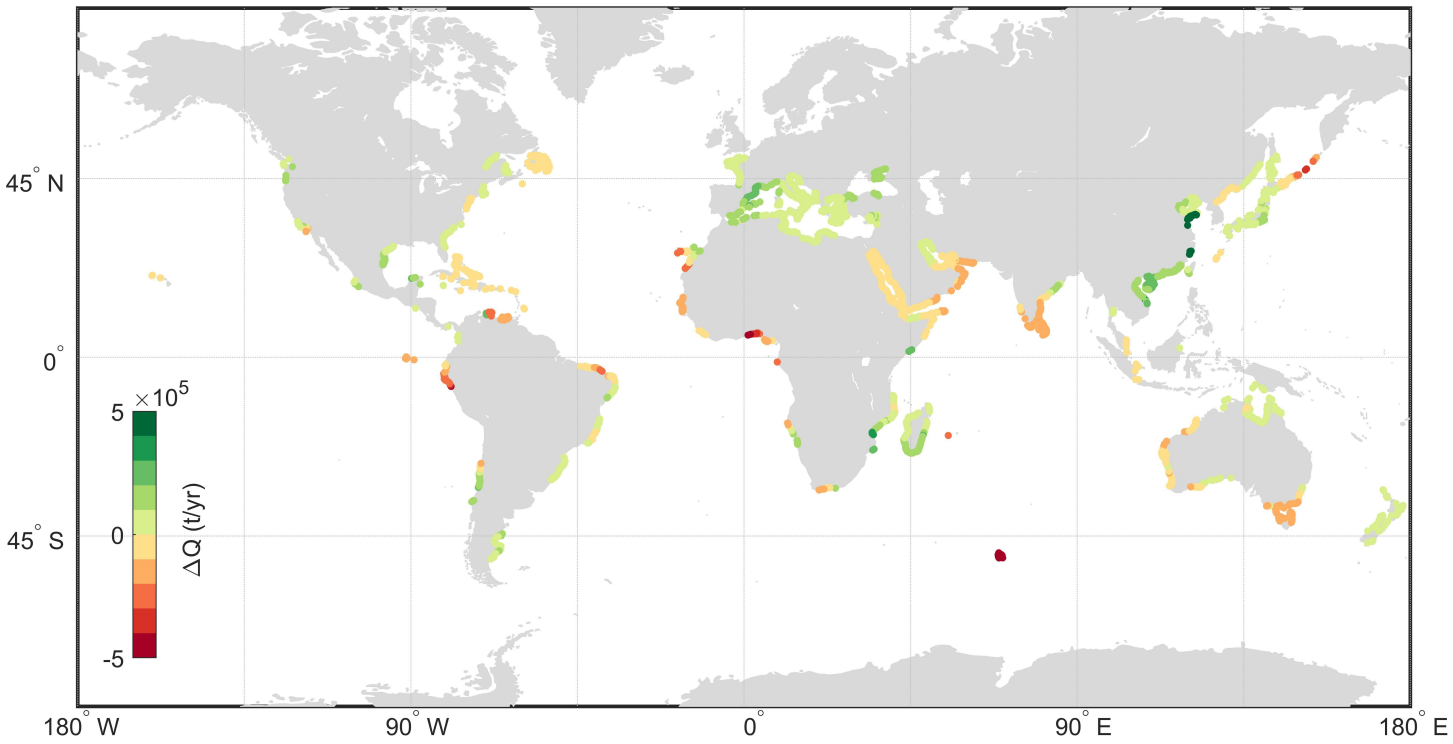

Figure 3: **Modelled sediment imbalance.** Global geographic distributions of the modelled sediment imbalance for sandy coasts for which the high frequency evolution of the coastline is considered to be potentially dominated by the imbalance of the sand budget ($\xi < 0.9$, see Methods).

Influences on terrestrial supply: the impact of river dams

Researchers have long discussed the impact of anthropogenic activities on river sediment supply [27, 34]. Surprisingly, its effect, although described by authors, has not been taken into general consideration and is overlooked by the community studying beach dynamics.

In order to assess this anthropogenic effect, we have calculated the global picture for a world in which dams trap all the incoming sediment and for a pristine world without dams (see Methods). These two models are end-members. The model with dams is extreme, as the sediment trapping efficiency is quite variable, mainly depending on the water residence time[35, 36], usually >50% and sometimes up to 100% (example of the Aswan Dam on the Nile[37]). The difference between these two scenarios is shown in Figure 4. It shows that a dam retention capacity of 100% would reduce the overall Q_{river} by half, from 600,000 cubic metres in a pristine world to 270,000 cubic metres per year per transect on average in a world where dams retain all the sediments, thus depriving the coastal system of half of its sediment supply. Note that these values consistently bracket the current value estimated by the BQART model (400,000 cubic metres per year per transect). In this tested scenario, 18% of the sandy transects ($n = 454$, i.e. approximately 23,000 km of coastline) with a neutral or positive sand budget become sediment deficient once the dams are taken into account. Although extreme, this scenario illustrates the potential effect of dams and provides pertinent information on the location of coastal areas affected by sedimentary input loss (Figure 4). Sediment loss is critical for especially large deltas, which are fragile areas mostly formed from river sediment supply [11, 38, 39].

The effects of river sediment loss sometimes extend beyond the delta area and become regionally pervasive, as is the case along the Gulf Coast of the United States[40] where the multiplication of dams has led to a significant reduction in the supply of sediments from the Mississippi River to the coasts. In the last forty years, this has resulted in some of the highest rates of erosion in the state of Louisiana, as well hundreds of kilometres further to Texas and Florida[41].

One implication of these results is that a local modification in a catchment can have repercussions on the sandy coast evolution far away along the continental cell.

Limitations and way forward

Although the sand budget plays a primary role in the evolution of the coastline on a global scale, other phenomena, natural or not, can influence this evolution on different spatial and temporal scales. The contribution of these phenomena is difficult to quantify because global databases (e.g. high-resolution offshore topographic data or a subsidence map) are still lacking. Among these various phenomena, the global rise in sea level over the last 100 years has had a visible impact on beaches,

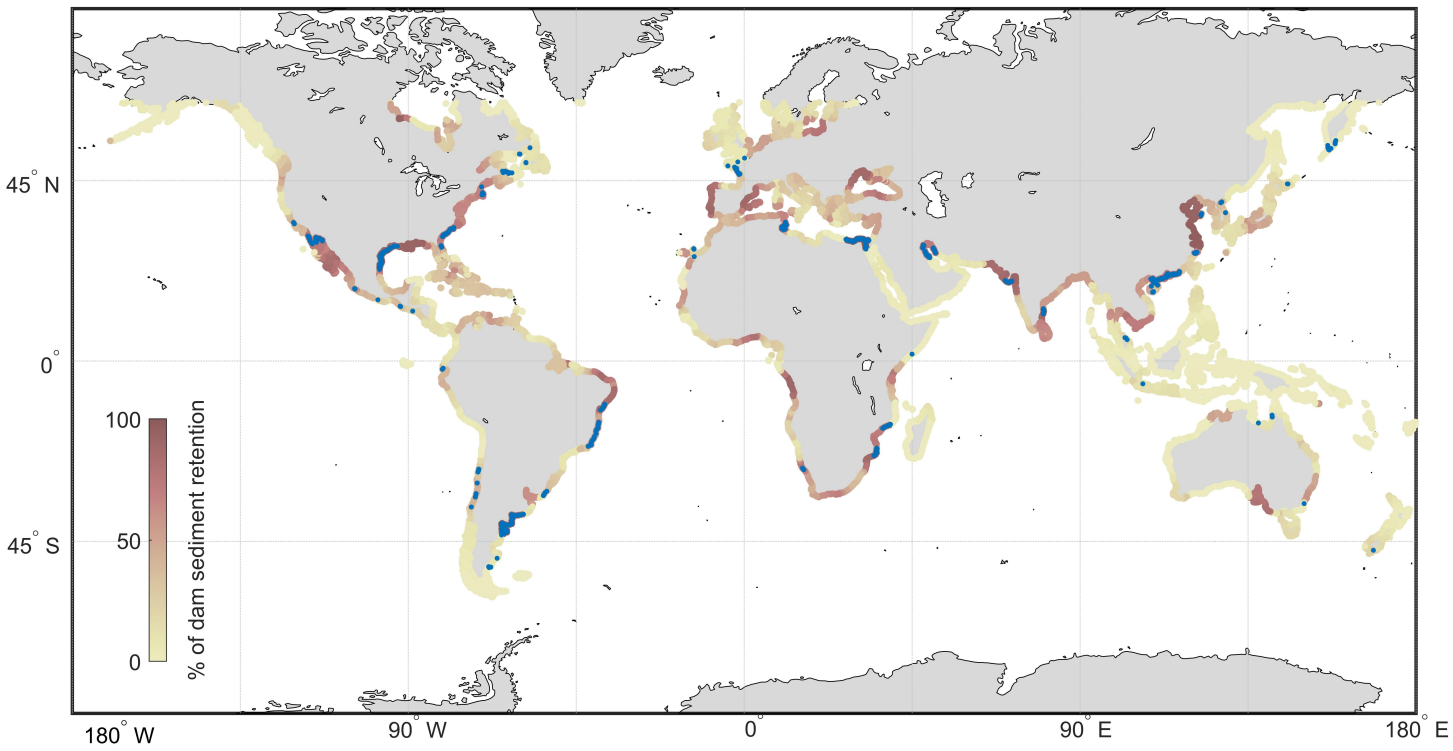

Figure 4: **Dam-induced relative sediment retention.** Global geographic distributions of the percentage of decrease in Q_{river} due to the presence of dams in catchments, assuming that dams retain all the sediment coming from upstream. The blue dots represent transects where the sand budget shifts from positive or neutral to a deficit once the dams are taken into account.

especially along gently sloping low-lying coasts. With a 25 cm rise in the sea level since 1900[1], the sea has gained up to 15 metres on land for beaches with a slope of 1 degree. For the future, with an accelerating sea level rise, studies predict that half of the world's beaches could disappear by 2100[8], although this underestimates the potential for coastal resilience[9] due to sediment availability. Local subsidence due to sediment compaction following freshwater pumping can reach several metres like in Japan or Indonesia[42], greatly exceeding any other cause for coastline evolution. Abrupt or transient vertical movement associated with the seismic cycle along subduction zones is another factor that can be responsible for metric to centimetric vertical uplift or subsidence over a period of years[43]. The whole of these phenomena are not quantified everywhere and may explain the remaining variance in the current sandy beach trend υ_{obs} that is not explained by ΔQ. There is still considerable unacceptable uncertainty about what the world's coasts will look like at the end of the century under different scenarios.

Nevertheless, our study constitutes a major breakthrough by providing the first evidence that the current trend in sandy coastal evolution is also controlled by the local imbalance of sand transport in a predictive way. Sediment supplied by rivers plays a crucial role in this imbalance and any variation in this supply, caused by dams for example, can affect sediment redistribution along continental cells. Variations in the river sediment supply are dependent on climate change. The rise in temperature[44] will increase the sediment transport potential of rivers as temperature directly affects the capacity of the river to erode the bed[45]. The intensification (rarefaction) of precipitation in temperate (arid) zones will lead to an increase (decrease) in Q_{river}[46]. Last, the multiplication of extreme climatic events (i.e. strong droughts, monsoons, etc.) will make the land vulnerable to erosion and thus influence sediment transport; a monsoon after a strong drought mobilizes large quantities of sediments. Dams are not the only anthropogenic factor to be considered with regards to the evolution of Q_{river}. Land use changes also have a critical role to play in the delivery of river sediment supply to the coast. Urbanization can hamper sediment transport, particularly through the increase in infrastructure along rivers and coasts. Conversely, deforestation and land use in general may also help increase Q_{river} by increasing the exposure of deforested soils to precipitation and the erodibility of soils that do not have enough tree roots to provide support[47].

Moving toward coastal zone sand management practices at the sand cell level

Our results show that the main threat for sandy coasts may come from a river sediment supply deficit that will be compounded by a rise in the sea level in the future. While the inertia of a global mean sea level rise is too large to be reversed in the 21st century, a sediment unbalance occurs on a local-to-regional scale and can either increase or decrease the coastal impacts of

rising seas [9] Local examples have shown that sandy coasts were rapidly reconstructed after river dam removal [38]. However, such actions must be based on conservation and integrated policies, a trade-off at the nexus of sustainable coastal areas.

Past experience has shown that effective, site-specific coastal planning can mitigate beach erosion and result in a stable coastline; the most prominent example of this is the Dutch coast[48]. While sea level rise results in coastal recession almost everywhere around the world, many locations have ambient erosive trends related to human interventions that could theoretically be avoided by more sustainable coastal and watershed management practices[49, 20, 50]. At the same time, the magnitude of the projected sea level rise implies unprecedented pressure on our coasts, requiring the development and implementation of informed and effective adaptation measures. At local scales, human activities can also directly affect the coastline, both in terms of erosion and accretion. Some countries such as China or the Netherlands are undertaking large-scale works to gain ground on the sea. Conversely, some countries (China, India, the USA, etc.) use their beaches as sand quarries to supply the construction industry. Land subsidence due to agriculture, mining, or urban development[13, 51], as well as coastal infrastructure, can be a dominant factor in coastal evolution[42]. This was recently highlighted by the decision to move the capital of Indonesia, given the impossibility of sustainably protecting Jakarta, the current capital, from marine flooding [42].

However, all these site-specific mitigation cases have neglected the sediment imbalance that results from larger scale, often regional, sediment redistribution[52]. Our study strongly suggests that the most efficient management strategies cannot be limited to a local scale. Our study highlights that a modification of the sediment supply by a river, which generally traverses several countries, can have repercussions far away along the coast up to thousands of kilometres (e.g. Namibian coast), depending on the coastal sediment cell. For example, the Bight of Benin, located in the Gulf of Guinea, West Africa, is under the influence of sediment supplied by the Volta and Niger rivers, and this sediment is redistributed along the coast. However, several agriculture and hydro-power dams were constructed on these rivers, as well as deep water harbours, blocking the transport of sediment downstream. Although some countries are implementing expensive mitigation strategies locally, a collaborative international effort would certainly deliver more benefits [53, 54] with a reduced cost [55]. This teleconnection must be considered in coastal management. Although current legislation does not take the integrated analysis of continental and offshore sources of sediments into account, our study suggests that it is possible to act on the evolution of sandy coasts controlled by the sediment imbalance, for example by managing the sediment retention by dams or adapting land use policies at a regional-to-continental scale. Given that the change in sediment outflux from one river may impact the shorelines of another country, we anticipate that integrated and comprehensive approaches such as the one proposed for the first time in our study could have consequences both for national coastal management policies and for international legislation.

Methods

Coastal transects and their mass budget, ΔQ

For the coastline, we use the Global Self-consistent Hierarchical High-resolution Geography Database (GSHHG version 2.3.6 August 17, 2016)[56]. The GSHHG coastline is segmented into points representing 50-km long entities called transects. The code used to solve the sand imbalance along the coast is a 1D code linking successive transects along the coast by calculating the following mass budget:

$$\Delta Q = R_{cross} Q_{in} - Q_{out} = R_{cross}(Q_{river} + Q_{wave,in}) - Q_{wave,out} \tag{2}$$

where V is the volume of sediment in m^3, R_{cross} is the cross-shore transport rate, Q_{river} is the annual fluvial solid discharge into the transect in $kg/year$, and $Q_{wave,in}$ (respectively $Q_{wave,out}$) is the wave-induced longshore sediment transport flux, in $kg/year$, coming from the previous transect (respectively going to the next transect). R_{cross} is calculated as $R_{cross} = 2 \times min(1, DoC_i/l_c) - 1$, where DoC_i is the local depth of closure and l_c is a characteristic length.

River sediment supply, Q_{river}

The annual river sediment discharge, represented by the variable Q_{river}, has been calculated using the BQART[45] formula (see Equation 3). It works for catchments and therefore we used it for every catchment flowing to the ocean, as defined in the HydroBASIN database[57]. In the HydroBASIN database, small streams that drain directly to the coast are aggregated into entities of the order of 100 km^2 (max 500 km^2). In the absence of a better solution, we applied BQART on these surfaces, even if BQART has not been validated in this case.

$$Q_{river} = \omega B Q^{0.31} A^{0.5} R. \max(T, 2) \tag{3}$$

where $\omega = 0.0006$[45], Q_{river} is the solid river discharge in $Mt/year$, T is the average ambient temperature ($^\circ C$), Q is the liquid river discharge ($km^3/year$), A is the drainage area of the catchment (km^2) and R is the relief (i.e. the difference in elevation from highest catchment point and its outlet, in km). In addition, $B = IL(1 - T_E)E_H$ accounts for geological as

well as human factors[45]. In the formulation of B, I is a modulation from glacier erosion: $I = 1 + 0.09A_g$ where A_g is the percentage area covered by glaciers. L is a lithological factor usually in the range of 0.5 (low erodibility lithology) to 3 (high erodibility lithology). T_E is the fraction of sediment trapped in lakes, whether natural or anthropogenic; it amounts to 0-1, with a probable global average of 0.2[45](value used for the calculation). Last, E_H is an anthropic factor, and can have one of three possible values: $E_H = 0.5$ for areas with conservative human footprints (density $< 200\ inh./km^2$, and gross domestic product per capita$>$ 15000 $\$/yr$); $E_H = 2$ for areas with high human footprints (density $> 200\ inh./km^2$, and gross domestic product per capita$<$ 1000 $\$/yr$); or $E_H = 1$, for areas with low human footprints.

In order to calculate Q_{river} with the BQART formula, we extracted the values of Q, A, R, T, A_g, *population density*, and *gross domestic product per capita* from the HydroBASIN database[57]. L is determined from the lit_cl_smj categories in the GLiM database[58].

In the BQART model, the effect of dams is lumped into the T_E parameter, but T_E is poorly constrained, and includes potential sediment storage in plains. The same value was used for all the catchments and corresponds to a worldwide mean of 0.2[45]. In order to better evaluate the impact of dams on the sediment flux in different catchments, we used a model where the sediment flux can be calculated on every pixel and either summed or partially removed by dams in order to calculate the sediment outflux to the ocean Q_{river}. This model was proposed by Maffre et al.[26] on the basis of a 3.75◦ longitude by 1.9◦ latitude grid of cells:

$$E = kq^{0.2}s^{1.3}max(T, 2)^{0.9} \tag{4}$$

where E is the pixel erosion rate in $m/year$, k is a constant parameter adjusted to obtain a global sediment outflux of 19 Gt (as predicted by the BQART model), s is the local slope, q is the run-off ($mm/year$) and T is the ambient temperature in ($^{\circ}C$). Erosion rates are summed within catchments in order to predict the sediment flux Q_{river} at their outlet.
To quantify the impact of dams on Q_{river}, we used the GOODD dam database[59], which provides the location of the dams as well as the associated upstream watersheds. We calculated $Q_{river,dam}$ by masking the area upstream from the dams, so that it mimics total sediment retention in dam reservoirs assuming that 100% of the sediment is trapped. Overall, $Q_{river,dam}$ fits Q_{river} calculated by using the BQART with a correlation coefficient of $R = 0.76$. We also calculated a pristine $Q_{river,p}$ assuming a world without dams and using Equation 4, so that we can compare the two situations with respect to the sandy coast evolution.

Because our model focuses on sand, we consider that only 35% of the total riverine sediment input is sand reaching the coastal zone[60] and that this sand has a median diametre of $d_{50} = 400\mu m$.

Longshore wave-induced sand transport, Q_{wave}

The empirical wave-induced longshore sediment transport is based on hydrological and topographic data and calculated using the Kamphuis formula (Equation 5). We consider a single grain size of $d_{50} = 400\mu m$ which corresponds to intermediate-sized sand, with an underwater beach slope of $tan(\beta) = 0.1$[61]. T_p is the peak wave period in s, H_{break} is the wave height at the breaker line in m and θ_{break} is the wave angle at the breaker line in degrees. The average wave regime was derived from Era-Interim (ECMWF) over the 1993-2015 period.

$$Q_{wave} = 2.33T_p^{1.5}tan(\beta)^{0.75}d_{50}^{-0.25}H_{break}^2sin(2\theta_{break})^{0.6} \tag{5}$$

According to the relative angle between the waves and shoreline, transport occurs in either one direction or the other. A set of consecutive transects where the transport moves in the same direction constitutes a hydrosedimentary cell. Within a cell, each transect receives sand from the previous transect and supplies sand to the next transect. At each of the two extremities of the cell, the sand either converges (accretion) or diverges (erosion).

Islands are considered as isolated coastal systems; there is no sand flux from one island to another. The model provides results in one iteration starting from a hypothetical initial situation where sandy beaches are infinite reservoirs of detached sand and non-sandy stretches of coast are empty reservoirs. Here, the sandy transects were delineated as in the database of Luijendijk et al.[2]

Sand loss towards the ocean, R_{cross}

To take the sand outflux from the coast to the ocean into account, we determined a cross-shore 'rate' for each transect. This rate was developed to model seaward sand sinks, the direct drift of sand from river outlets to the open ocean and wave-induced

drift.

The parameter DoC_i/l_c, where l_c is a characteristic length, controls the value of this rate. It was adjusted to maximize the correlation between the modelled sand budget ΔQ and the observed erosion trends υ_{obs}[2], and the resulting value is $l_c = 8.5m$ which is approximately equal to the average value of the DoC at the global scale[30]. A rate close to -1 means that the system loses twice as much sand locally through cross-shore transport as it receives through riverine and coastal transport. Conversely, a rate close to 1 means that a negligible part of the input drifts offshore.

ϵ_{obs} vs. ΔQ correlation: ξ definition and breaking down the dataset into subsets

After calculating the sand budget on each transect, we applied a sliding average filter with a radius of 5° to the results in order to smooth them out and to highlight the overall patterns. Points found at latitudes above 50° (north and south) were excluded as they correspond to areas such as Patagonia or Northern Canada where the model fails to properly represent sand transport, probably due to the multitude of closely interspaced islands.
The metric ξ has been defined in order to quantify how the high-frequency shoreline evolution is correlated to the sand budget (ΔQ). We assume that, for an ideal beach constrained only by sand supply, the shoreline evolves linearly with the sand budget. In other words, high-frequency shoreline evolution (erosion or accretion) is represented by ϵ_{obs}. Thus, ξ is defined as the relative difference of $\mid \Delta Q \mid \epsilon_{obs}$ from its reference value given by the ratio of global average values $\mid \overline{\Delta Q} \mid \overline{\epsilon_{obs}}$; it is non-dimensional:

$$\xi = \left| \frac{\mid \Delta Q \mid \epsilon_{obs}}{\mid \overline{\Delta Q} \mid \overline{\epsilon_{obs}}} - 1 \right|$$

Considering the normalized value $\Delta Q^* = \mid \Delta Q \mid / \overline{\mid \Delta Q \mid}$ versus the normalized value $\epsilon^*_{obs} = \epsilon_{obs}/\overline{\epsilon_{obs}}$, $\xi = 0$ means $\Delta Q^* = \epsilon^*_{obs}$ i.e. a perfect linear regression between ϵ^*_{obs} and ΔQ^*. When ξ is higher, the difference between normalized ϵ_{obs} and $\mid \Delta Q \mid$ is also higher; this difference follows the rule $\Delta Q^* = (1 \pm \xi) \times \epsilon^*_{obs}$. We define a threshold value ξ_c for ξ in order to select the transects that do not deviate too much from the perfect linear regression between ϵ^*_{obs} and ΔQ^*. $\xi_c = 0.9$ satisfies this constraint, without being too restrictive. The threshold value $\xi_c = 0.9$ also ensures that the variability in the evolution of the coastline ϵ_{obs} is comparable to that expected from the value of ΔQ.

$$\Delta Q^* \in [(1-\xi_c) \times \epsilon^*_{obs} \ ; \ (1+\xi_c) \times \epsilon^*_{obs}] \ \Leftrightarrow \ \Delta Q^* \in [0.1 \times \epsilon^*_{obs} \ ; \ 1.9 \times \epsilon^*_{obs}] \ \textit{considering} \ \xi_c = 0.9$$

Based on the definition of ξ and the nature of coastal transects described in *Luijendijk et al.*[2], we produced the four subsets of transects defined in Table 1. These subsets are working subsets upon which we test the correlation between the observed annual coastline evolution trend υ_{obs}[2] and our calculated ΔQ.

Symbol	Condition	Description	N	R
A	-	Entire dataset	11161	-0.024
B	Sandy	Sandy coastlines[2]	3916	0.064
C	$\xi < 0.9$	all the transects where ϵ_{obs} correlates with $\lvert\Delta Q\rvert$	6498	0.381
D	Sandy & $\xi < 0.9$	Sandy coastlines[2] where ϵ_{obs} correlates with $\lvert\Delta Q\rvert$	2506	0.588

Table 1: Subset characteristics, and results of the analysis: N is the total transect number and R the correlation coefficient between υ_{obs} and ΔQ.

References

[1] M. Oppenheimer, B.C. Glavovic, J. Hinkel, R. van de Wal, A.K. Magnan, A. Abd-Elgawad, R. Cai, M. Cifuentes-Jara, R.M. DeConto, T. Ghosh, J. Hay, F. Isla, B. Marzeion, B. Meyssignac, and Z. Sebesvari. Sea level rise and implications for low-lying islands, coasts and communities. *IPCC Special Report on the Ocean and Cryosphere in Changing Climate*, 2019.

[2] A. Luijendijk, G. Hagenaars, R. Ranasinghe, F. Baart, G. Donchyts, and Stefan Aarninkhof. The state of the world's beaches. *Scientific Reports*, 2018.

[3] P. Bruun. Sea level rise as cause of shore erosion. *Journal of Waterways and Harbor Division*, ASCE 88:117–130, 1962.

[4] R.G Dean. Beach response to sea level change. *Ocean Engineering Science*, v.9 of The Sea:869–887, 1990.

[5] S.P et al. Leatherman. Sea level rise shown to drive coastal erosion. *Transactions of the American Geophysical Union*, 81 (6):55–57, 2000.

[6] J.D. Rosati, R.G. Dean, and T.L. Walton. The modified bruun rule extended for landward transport. *Marine Geology*, 340:71–81, 05 2013.

[7] C.H. Everts. Sea level rise effects. *Journal of Waterway, Port, Coastal and Ocean Engineering, American Society of Civil Engineers*, 111 (6):985–999, 1985.

[8] Michalis I. Vousdoukas, Roshanka Ranasinghe, Lorenzo Mentaschi, Theocharis A. Plomaritis, Panagiotis Athanasiou, Arjen Luijendijk, and Luc Feyen. Sandy coastlines under threat of erosion. *Nature Climate Change*, 10:260–263, 2020.

[9] J.A.G Cooper, Gerd Masseling, Giovanni Coco, Andrew Short, Bruno Castelle, K. Rogers, Edward J. Anthony, A.N. Green, J.T. Kelley, O.H. Pilkey, and D.W.T. Jackson. Sandy beaches can survive sea-level rise. *Nature Climate Change*, October 2020.

[10] Sean Vitousek, Patrick L. Barnard, and Patrick Limber. Can beaches survive climate change? *Journal of Geophysical Research: Earth Surface*, 122(4):1060–1067, 2017.

[11] J.H. Nienhuis, A.D. Ashton, and D.A. et al. Edmonds. Global-scale human impact on delta morphology has led to net land area gain. *Nature*, 577:514–518, 2020.

[12] James Syvitski, Scott Peckham, Rachael Hilberman, and Thierry Mulder. Predicting the terrestrial flux of sediment to the global ocean: a planetary perspective. *Sedimentary Geology*, 162(1-2):5–24, November 2003.

[13] Patrick Marchesiello, Nguyet Minh Nguyen, Nicolas Gratiot, Hubert Loisel, Edward J. Anthony, Cong San Dinh, Thong Nguyen, Rafael Almar, and Elodie Kestenare. Erosion of the coastal mekong delta: Assessing natural against man induced processes. *Continental Shelf Research*, 2019.

[14] C. B. Craft, E. D. Seneca, and S. W. Broome. Vertical Accretion in Microtidal Regularly and Irregularly Flooded Estuarine Marshes. *Estuarine, Coastal and Shelf Science*, 37(4):371–386, October 1993.

[15] Mohsen Taherkhani, Sean Vitousek, Patrick L. Barnard, Neil Frazer, Tiffany R. Anderson, and Charles H. Fletcher. Sea-level rise exponentially increases coastal flood frequency. *Scientific Reports*, 10(6466), 2020.

[16] R. Ranasinghe. On the need for a new generation of coastal change models for the 21st century. *Sci Rep*, 10, 2010, 2020.

[17] Jérôme Benveniste, Anny Cazenave, Stefano Vignudelli, Luciana Fenoglio-Marc, Rashmi Shah, Rafael Almar, Ole Andersen, Florence Birol, Pascal Bonnefond, Jérôme Bouffard, Francisco Calafat, Estel Cardellach, Paolo Cipollini, Gonéri Le Cozannet, Claire Dufau, Maria Joana Fernandes, Frédéric Frappart, James Garrison, Christine Gommenginger, Guoqi Han, Jacob L. Høyer, Villy Kourafalou, Eric Leuliette, Zhijin Li, Hubert Loisel, Kristine S. Madsen, Marta Marcos, Angélique Melet, Benoît Meyssignac, Ananda Pascual, Marcello Passaro, Serni Ribó, Remko Scharroo, Y. Tony Song, Sabrina Speich, John Wilkin, Philip Woodworth, and Guy Wöppelmann. Requirements for a coastal hazards observing system. *Frontiers in Marine Science*, 6:348, 2019.

[18] A. Melet, P. Teatini, G. Le Cozannet, C. Jamet, A. Conversi, J. Benveniste, and Rafael Almar. Earth observations for monitoring marine coastal hazards and their drivers. *Surveys in Geophysics*, [Early access]:p. [46 p.], 2020.

[19] R. Ranasinghe. On the need for a new generation of coastal change models for the 21st century. *Sci Rep*, 2020.

[20] T. Tiggeloven, H. de Moel, H. C. Winsemius, D. Eilander, G. Erkens, E. Gebremedhin, A. Diaz Loaiza, S. Kuzma, T. Luo, C. Iceland, A. Bouwman, J. van Huijstee, W. Ligtvoet, and P. J. Ward. Global-scale benefit–cost analysis of coastal flood adaptation to different flood risk drivers using structural measures. *Natural Hazards and Earth System Sciences*, 20(4):1025–1044, 2020.

[21] John Milliman and Katherine Farnsworth. Runoff, erosion, and delivery to the coastal ocean. *River Discharge to the Coastal Ocean: A Global Synthesis*, page 43, 01 2011.

[22] Robert J. Hallermeier. Uses for a calculated limit depth to beach erosion. *Coastal Engineering 1978*, pages 1493–1512, 1978.

[23] Edward J. Anthony and Troels Aagaard. The lower shoreface: Morphodynamics and sediment connectivity with the upper shoreface and beach. *Earth-Science Reviews*, 2020.

[24] Nieves G. Valiente, Gerd Masselink, Tim Scott, Daniel Conley, and Robert Jak McCarroll. Role of waves and tides on depth of closure and potential for headland bypassing. *Marine Geology*, 407:60–75, 2019.

[25] Kamphuis. Alonshore sediment transport rate. *Coastal and Oc. Engrg.*, 117:624–640, 1991.

[26] P. Maffre. a. *a*, a:a, a.

[27] Jaia Syvitski and John Milliman. Geology, geography, and humans battle for dominance over the delivery of fluvial sediment to the coastal ocean. *Journal of Geology*, 115, 01 2007.

[28] James Syvitski and Albert Kettner. Sediment flux and the Anthropocene. *Philosophical Transactions of the Royal Society A: Mathematical, Physical and Engineering Sciences*, 369(1938):957–975, 2011.

[29] Bernhard Peucker-Ehrenbrink. Land2sea database of river drainage basin sizes, annual water discharges, and suspended sediment fluxes. *Geochemistry, Geophysics, Geosystems*, 10(6), June 2009.

[30] Erwin W.J. Bergsma and Rafael Almar. Coastal coverage of esa' sentinel 2 mission. *Advances in Space Research*, 65(11):2636 – 2644, 2020.

[31] Jonathan A. Warrick. Littoral sediment from rivers: Patterns, rates and processes of river mouth morphodynamics. *Frontiers in Earth Science*, 8:355, 2020.

[32] Liviu Giosan, Stefan Constantinescu, Peter D. Clift, Ali R. Tabrez, Muhammed Danish, and Asif Inam. Recent morphodynamics of the indus delta shore and shelf. *Continental Shelf Research*, 26(14):1668–1684, 2006.

[33] Cope M. Willis and Gary B. Griggs. Reductions in Fluvial Sediment Discharge by Coastal Dams in California and Implications for Beach Sustainability. *The Journal of Geology*, 111(2):167–182, March 2003.

[34] John Milliman and M. Ren. River flux to the sea: impact of human intervention on river systems and adjacent coastal areas. *Impact on coastal habitation*, pages 57–83, 1995.

[35] Eric Maneux, Jean Luc Probst, Eric Veyssy, and Henri Etcheber. Assessment of dam trapping efficiency from water residence time: Application to fluvial sediment transport in the Adour, Dordogne, and Garonne River Basins (France). *Water Resources Research*, 37(3):801–811, March 2001.

[36] Guangming Tan, Peng Chen, Jinyun Deng, Quanxi Xu, Rouxin Tang, Zhiyong Feng, and Ran Yi. Review and improvement of conventional models for reservoir sediment trapping efficiency. *Heliyon*, 5(9):e02458, September 2019.

[37] DE Walling and BW Webb. Erosion and sediment yield: a global overview. *IAHS Publications-Series of Proceedings and Reports-Intern Assoc Hydrological Sciences*, 236:3–20, 1996.

[38] J.A. Warrick, A.W. Stevens, and I.M. et al. Miller. World's largest dam removal reverses coastal erosion. *Sci Rep*, 2019.

[39] SH Sharaf El Din. Longshore sand transport in the surf zone along the mediterranean egyptian coast. *Limnology and Oceanography*, 19(2):182–189, 1974.

[40] L. Mentaschi, M.I. Vousdoukas, and JF. et al. Pekel. Global long-term observations of coastal erosion and accretion. *Sci Rep*, 2018.

[41] Robert A. Morton, Tara Miller, and Laura Moore. Historical Shoreline Changes Along the US Gulf of Mexico: A Summary of Recent Shoreline Comparisons and Analyses. *Journal of Coastal Research*, 2005(214):704 – 709, 2005.

[42] Anh Cao, Miguel Esteban, Ven Paolo Bruno Valenzuela, Motoharu Onuki, Hiroshi Takagi, Nguyen Danh Thao, and Nobuyuki Tsuchiya. Future of Asian Deltaic Megacities under sea level rise and land subsidence: current adaptation pathways for Tokyo, Jakarta, Manila, and Ho Chi Minh City. *Current Opinion in Environmental Sustainability*, 50:87–97, June 2021.

[43] M. Farías, G. Vargas, A. Tassara, S. Carretier, S. Baize, D. Melnick, and K. Bataille. Land-level changes produced by the mw 8.8 2010 chilean earthquake. *Science*, 2005(329), 2010.

[44] O. Hoegh-Guldberg, D. Jacob, M. Taylor, M. Bindi, S. Brown, I. Camilloni, A. Diedhiou, R. Djalante, K.L. Ebi, F. Engelbrecht, J. Guiot, A. Payne S.I. Seneviratne A. Thomas R. Warren Y. Hijioka, S. Mehrotra, and G. Zhou. Impacts of 1.5ºc global warming on natural and human systems. *IPCC Report*, 2018.

[45] James P. M. Syvitski and John D. Milliman. Geology, Geography, and Humans Battle for Dominance over the Delivery of Fluvial Sediment to the Coastal Ocean. *The Journal of Geology*, 115(1):1–19, January 2007.

[46] P. Greve, L. Gudmundsson, and S.I. Seneviratne. Regional scaling of annual mean precipitation and water availability with global temperature change. *Earth System Dynamics*, 9:227–240, 2018.

[47] J.D. Restrepo, A.J. Kettner, and J.P.M. Syvitski. Recent deforestation causes rapid increase in river sediment load in the colombian andes. *Anthropocene*, pages 13–28, 10 2015.

[48] Jan P.M. Mulder, Saskia Hommes, and Erik M. Horstman. Implementation of coastal erosion management in the netherlands. *Ocean & Coastal Management*, 54(12):888–897, 2011. Concepts and Science for Coastal Erosion Management (Conscience).

[49] R.L. Morris, A. Boxshall, and S.E. Swearer. Climate-resilient coasts require diverse defence solutions. *Nat. Clim. Chang.*, (10):485–487, 2020.

[50] Daniel Lincke and Jochen Hinkel. Coastal migration due to 21st century sea-level rise. *Earth's Future*, 9(5), 2021.

[51] Robert J. Nicholls, Daniel Lincke, Jochen Hinkel, Sally Brown, Athanasios T. Vafeidis, Benoit Meyssignac, Susan E. Hanson, Jan-Ludolf Merkens, and Jiayi Fang. A global analysis of subsidence, relative sea-level change and coastal flood exposure. *Nat. Clim. Chang.*, 11:338–342, 2021.

[52] Rafael Almar, Elodie Kestenare, J. Reyns, Julien Jouanno, E. J. Anthony, R. Laibi, M. Hemer, Yves Penhoat du, and R. Ranasinghe. Response of the Bight of Benin (Gulf of Guinea, West Africa) coastline to anthropogenic and natural forcing : Part 1 : Wave climate variability and impacts on the longshore sediment transport. *Continental Shelf Research*, 110:48–59, 2015.

[53] B. Alves, D. B. Angnuureng, Pierre Morand, and Rafael Almar. A review on coastal erosion and flooding risks and best management practices in West Africa : what has been done and should be done. *Journal of Coastal Conservation*, 24:art. 38 [22 p.], 2020.

[54] Olusegun Dada, Rafael Almar, Pierre Morand, and Frédéric Ménard. Towards West African coastal social-ecosystems sustainability : Interdisciplinary approaches. *Ocean and Coastal Management*, May 2021.

[55] Nicolas Rocle, HELENE REY-VALETTE, François Bertrand, Nicolas Becu, Nathalie Long, Cécile Bazart, Didier D. Vye, Catherine Meur-Ferec, Elise Beck, Marion Amalric, and Nicole Lautrédou-Audouy. Paving the way to coastal adaptation pathways: An interdisciplinary approach based on territorial archetypes. *Environmental Science and Policy*, 110:34–45, August 2020.

[56] P. Wessel and W. H. F. Smith. A global self-consistent, hierarchical, high-resolution shoreline database. *J. Geophys. Res.*, 101, 1996.

[57] B. Lehner and Grill G. Global river hydrography and network routing: baseline data and new approaches to study the world's large river systems. www.hydrosheds.org, 2013.

[58] Jens Hartmann and Nils Moosdorf. The new global lithological map database GLiM: A representation of rock properties at the Earth surface. *Geochemistry, Geophysics, Geosystems*, 13(12), 2012.

[59] M. Mulligan, A. van Soesbergen, and L. Saenz. GOODD, a global dataset of more than 38,000 georeferenced dams, 2020.

[60] L. D. Wright and C. A. Nittrouer. Dispersal of river sediments in coastal seas: Six contrasting cases. *Estuaries*, 18(3):494–508, 1995.

[61] Fabrice Ardhuin and Aron Roland. Coastal wave reflection, directional spread, and seismoacoustic noise sources. *Journal of Geophysical Research: Oceans*, 117(C11), 2012.

Author contributions statement

M.G. carried out the study and wrote the initial draft. V.R. calculated the sediment supply from rivers at the global scale. All authors discussed the results and contributed to the manuscript.

Additional information

Accession codes and data

The raw data that support the findings of this study are already available online. Calculated data (e.g. sediment outfluxes) are provided as tables. The Matlab Code will be made freely available through gitlab repository.

Competing interests

The authors declare no competing interests.